Engineering a Fibrocartilage Spectrum Through Modulation of Aggregate Redifferentiation

Meghan K. Murphy,* Taylor E. Masters,* Jerry C. Hu,* and Kyriacos A. Athanasiou*†

*Department of Biomedical Engineering, University of California Davis, Davis, CA, USA
†Department of Orthopaedic Surgery, University of California Davis, Davis, CA, USA

Expanded costochondral cells provide a clinically relevant cell source for engineering both fibrous and hyaline articular cartilage. Expanding chondrocytes in a monolayer results in a shift toward a proliferative, fibroblastic phenotype. Three-dimensional aggregate culture may, however, be used to recover chondrogenic matrix production. This study sought to engineer a spectrum of fibrous to hyaline neocartilage from a single cell source by varying the duration of three-dimensional culture following expansion. In third passage porcine costochondral cells, the effects of aggregate culture duration were assessed after 0, 8, 11, 14, and 21 days of aggregate culture and after 4 subsequent weeks of neocartilage formation. Varying the duration of aggregate redifferentiation generated a spectrum of fibrous to hyaline neocartilage. Within 8 days of aggregation, proliferation ceased, and collagen and glycosaminoglycan production increased, compared with monolayer cells. In self-assembled neocartilage, type II-to-I collagen ratio increased with increasing aggregate duration, yet glycosaminoglycan content varied minimally. Notably, 14 days of aggregate redifferentiation increased collagen content by 25%, tensile modulus by over 110%, and compressive moduli by over 50%, compared with tissue formed in the absence of redifferentiation. A spectrum of fibrous to hyaline cartilage was generated using a single, clinically relevant cell source, improving the translational potential of engineered cartilage.

Key words: Costal chondrocytes; Monolayer expansion; Three-dimensional culture; Self-Assembly; Hyaline cartilage

INTRODUCTION

Articular cartilage degeneration affects a number of load-bearing joints including the knee, hip, shoulder, facet, and temporomandibular joint (TMJ). Based on the 2007–2009 National Health Interview Survey, 50 million Americans reported doctor-diagnosed arthritis, and 21 million experienced arthritis-related activity limitations (11). However, existing clinical approaches for articular cartilage degeneration seldom provide long-term repair and restoration of a healthy loading environment (14,29, 33). In the case of hyaline cartilage lesions, such approaches include debridement, in which the joint is arthroscopically cleaned of loose debris and surfaces are smoothed; microfracture, in which defects are created to initiate bleeding from the subchondral bone; and mosaicplasty, in which cartilage biopsies are removed from nonarthritic regions and pieced together to resurface the load-bearing regions. In the case of fibrocartilage degeneration, partial or total discectomy or meniscectomy may be used to remove a portion of the meniscus or the entire structure. Engineering a replacement tissue may present an alternate approach to replace degenerated tissues, circumventing the negative side effects and shortcomings of current standards of care (25).

Hyaline and fibrous cartilages are two distinctly different articular structures, both of which contribute to a healthy loading environment in diarthrodial joints. Hyaline cartilage, which lines the ends of long bones, plays a key role in the distribution of forces borne by the joint and reduces the coefficient of friction during motion. The predominant type of collagen in hyaline cartilage is type II collagen (90%), accompanied by an abundance of glycosaminoglycans (GAGs) (3). Unlike hyaline cartilage, fibrocartilage consists of predominantly type I collagen with minimal GAG content (3). Fibrocartilage is found in the knee meniscus, intervertebral disc, TMJ disc, and mandibular condyle. Fibrocartilage functions to distribute loads experienced by the surrounding structures. The collagen is highly organized, resisting strains along the functional axes. Though hyaline and fibrocartilages differ in their composition and structure, both are essential to joint function, but lack sufficient capacity for self-repair.

Tissue engineering has the potential to produce functional replacement tissue for addressing hyaline and fibrocartilage degeneration. The self-assembling process has been developed to engineer robust scaffold-free constructs (22). The self-assembling process entails seeding chondrocytes at high density (10^7 cells/ml) in nonadherent wells. The cells demonstrate cell–cell interactions within 24 h of seeding, and begin producing extracellular matrix (ECM) (38). This process is reminiscent of cartilage development and results in neocartilage with mechanical properties approaching those of native tissue (38). Moreover, manipulating cell source, culture conditions, and exogenous stimuli can enhance functional properties of engineered tissues. Efforts to engineer hyaline cartilage using articular chondrocytes in the self-assembling process have shown significant promise. In the presence of exogenous stimuli, tissue rich in type II collagen and GAGs, with tensile moduli over 3.5 MPa and an aggregate modulus of approximately 100 kPa, has been developed (36). Separately, efforts have shown that articular chondrocyte and meniscus cell cocultures may be used to engineer meniscus-shaped fibrocartilage with anisotropic tensile properties (Young's modulus over 3 MPa circumferentially, 2 MPa radially) (24). Common among these is the reliance on differentiated, articular chondrocytes, whose scarcity limits their use in autologous therapy. The ability to generate both hyaline and fibrous cartilage from a single, clinically relevant cell source would greatly improve the translational potential of tissue engineering efforts.

Costal cartilage exhibits notable potential as a cell source for tissue engineering. It is used in reconstructive surgeries, demonstrating isolation feasibility (35,47), and it is unaffected by pathologies of the diarthrodial joints (39). Expansion of chondrocytes has previously been shown to induce a shift toward a more fibrous phenotype (13,41). Compared with a spherical, chondrocyte-like morphology, cells exhibit a spread, fibroblast-like morphology with passage. This is accompanied by changes in matrix synthesis from type II collagen and aggrecan to fibroblastic matrices such as type I collagen (7,9,13). If methods are developed to direct and control this shift from one phenotype to the other, costal chondrocytes might hold the potential to generate both hyaline cartilage and fibrocartilage.

Informed by the articular cartilage literature, aggregate culture duration may present a method for manipulating costochondral cell phenotype, including matrix production, following monolayer expansion. Expanded chondrocytes have previously shown the potential to reexpress a chondrogenic phenotype upon reintroduction into the three-dimensional environment, which is valuable in engineering hyaline cartilage (5–7,26). Pellet cultures, polymer gels, and rotational cultures have all resulted in marked increases in cartilage-specific matrix expression following expansion (5–7,17,23,26,40). One such system, aggregate culture,

employs a single cell suspension (10^6 cells/ml) in a nonadherent dish, in rotation, allowing the cells to form suspended aggregates. In fourth passage articular chondrocytes, aggregate culture for 1 week significantly increased collagen and GAG content and tensile properties, compared with no aggregation and with pellet culture (23). Thus, varying the duration of aggregate culture may provide a useful means of engineering a spectrum of fibrous to hyaline cartilage using costal chondrocytes.

The present study sought to assess the effects of aggregate culture duration in third passage expanded costochondral cells. Using a one-factor analysis of variance study design, the effects of aggregate duration were assessed after 0, 8, 11, 14, and 21 days of aggregate culture and after 4 weeks of neocartilage formation. It was hypothesized that 1) in aggregates, increasing aggregate duration would increase type II to type I collagen ratio and GAG content; 2) in constructs, there is a beneficial aggregate culture duration that would increase overall collagen content, type II to type I collagen ratio, GAG content, and resulting mechanical properties; and 3) different types of cartilages may be obtained from differing aggregate durations. This work builds upon previous efforts to identify expansion conditions to enhance proliferation and maintain chondrogenic potential in third passage costochondral cells (34). The present study seeks to extend this effort by developing methods to manipulate the reexpression of the chondrogenic phenotype following monolayer. This may allow for the development of a fibrocartilaginous spectrum of engineered tissues.

MATERIALS AND METHODS

Cell Isolation and Expansion

Costal cartilage from crossbred Hampshire porcine approximately 6 months of age ($n = 4$, female, UC Davis Dept. Animal Sciences Meat Laboratory, Davis, CA, USA) were obtained within 24 h of death. A porcine model was selected based on translational efforts in the use of large animal models. Anatomically, there are notable similarities between the pig and the human, especially in the TMJ, as both are omnivores (27). Such similarities point to the pig as a model for allogeneic tissue replacements. Advantages include availability of skeletally mature tissue, though one disadvantage is variations in biomechanical loading in quadrupeds compared with bipedal humans.

Costal cartilage was isolated from the four caudal asternal ribs, and the perichondrium was discarded. Remaining cartilage was minced into 1-mm pieces and digested in 0.2% collagenase type II (Worthington, Lakewood, NJ, USA) in chemically defined chondrogenic culture medium (CHG) [Dulbecco's modified Eagle's medium with 4.5 g/L glucose and GlutaMAX (Gibco, Grand Island, NY, USA); 1% penicillin–streptomycin–fungizone (BD Biosciences, Bedford, MA, USA); 1% insulin, human transferrin, and

selenous acid (ITS+) premix (BD Biosciences); 1% non-essential amino acids (Gibco); 100 nM dexamethasone (Sigma, St. Louis, MO, USA); 50 µg/ml ascorbate-2-phosphate (Sigma); 40 µg/ml L-proline (Sigma); and 100 µg/ml sodium pyruvate (Sigma)] containing 3% fetal bovine serum (Atlanta Biologicals, Lawrenceville, GA, USA) for 18 h at 37°C. After digestion, the cell suspension was filtered, counted, and seeded in T-225 flasks (BD Biosciences) at 2.5×10^4 cells/cm^2. Cells were expanded in CHG supplemented with 1 ng/ml transforming growth factor (TGF)- 1 (PeproTech, Rocky Hill, NJ, USA), 5 ng/ml basic fibroblast growth factor (PeproTech), and 10 ng/ml platelet-derived growth factor (PeproTech) based on increases in proliferation and chondrogenic potential previously demonstrated by the authors in a study utilizing a separate costochondral cell batch (34). At 80–90% confluence, cells were passaged with 0.5% trypsin-ethylenediaminetetraacetic acid (EDTA) (Gibco) three times (P3). P3 was selected based on previous work investigating collagen and GAG synthesis in primary, P1, P3, and P5 costochondral cells. P3 cells demonstrated significantly greater GAG content with no significant differences in total collagen content compared with primary cells (1).

Chondrocyte Aggregation

Following monolayer expansion and prior to construct self-assembly, costochondral cells were redifferentiated in aggregate culture. The cells were seeded in a single cell suspension into 100-mm × 20-mm petri dishes (BD Biosciences) coated with 1% molecular biology-grade agarose (Fisher Scientific, Fair Lawn, NJ, USA) at 10^6 cells/ml CHG supplemented with 10 ng/ml TGF- 1. Dishes were placed on an orbital shaker at 72 rpm for 8 days, 11 days, 14 days, or 21 days. In the case of 0 days (no aggregation), cells were immediately seeded into constructs following the last passage. At the conclusion of the specified aggregation treatment, several aggregates were evaluated histologically. Remaining aggregates were digested for 45 min in 0.5% trypsin-EDTA, followed by 45 min in 0.2% collagenase type II on an orbital shaker at 37°C. Cell viability was assessed by trypan blue exclusion assay (Sigma).

The methods employed throughout the tissue engineering process are depicted in Figure 1.

Construct Formation

Constructs were self-assembled following aggregate digestion. A sterile, custom-made stainless steel mold consisting of 5-mm-diameter cylindrical prongs was constructed in-house to fit in six wells of a 48-well plate (Corning Inc., Corning, NY, USA). The wells were filled with 800 µl of sterile molten 2% molecular biology-grade agarose (Fisher Scientific) in phosphate-buffered saline (PBS, Sigma) and allowed to solidify at room temperature. Once the agarose solidified, the mold was removed, and CHG was used to saturate the wells prior to seeding. Cells were then seeded at 2×10^7 cells/ml in 100-µl aliquots. Thus, 2×10^6 cells were seeded into each 5-mm-diameter well. After 8 days of culture in the agarose wells, constructs were unconfined and placed in wells coated with a thin layer of 2% agarose to prevent adhesion. Unconfinement was intended to prevent radial growth restriction. Eight constructs were formed in each treatment. Constructs were cultured in CHG for a total of 4 weeks from seeding.

Histology

Both aggregates and constructs were analyzed histologically. Aggregate samples from each group were collected at the end of the specified treatment duration and construct samples were taken after 4 weeks of construct culture. Samples were frozen in HistoPrep Frozen Tissue Embedding Media (Fisher Scientific) and cryosectioned to 14 µm. Sections were fixed in formalin (EMD Chemicals, Gibbstown, NJ, USA) and stained with Safranin-O (Sigma)/fast-green (Sigma) for GAGs and with picrosirius red (Spectrum Chemical, Gardena, CA, USA) for collagen. Immunohistological staining techniques were used to detect the presence of types I and II collagen. Mouse anti-type I collagen monoclonal antibody at 1:600 dilution (Accurate Chemical, Westbury NY, USA) was used to detect type I collagen, and rabbit anti-human type II collagen polyclonal antibody at 1:200 dilution (Cedarlane Labs, Burlington, NC, USA) was used to detect type II collagen.
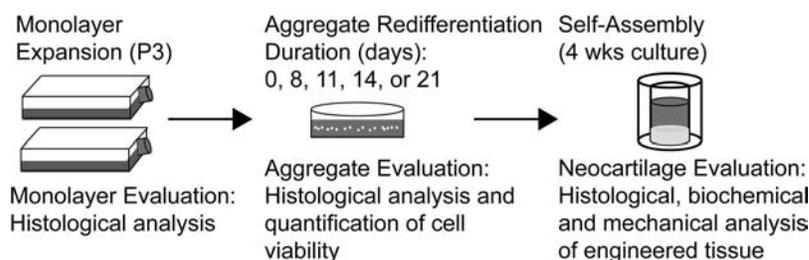
Figure 1. Neocartilage formation schematic. Costochondral cells were expanded to passage 3 (P3), and redifferentiated for 0 (immediately self-assembled), 8, 11, 14, or 21 days. Following redifferentiation, aggregates were digested, and cells were self-assembled.

Vectastain ABC mouse and rabbit secondary antibody staining kits (Vector Laboratories, Burlingame, CA, USA) were used to visualize types I and II collagen, respectively.

Biochemical Evaluation

Samples were analyzed for biochemical content after 4 weeks of construct culture. Samples were massed before and after 48 h of lyophilization and digested in 125 µg/ml papain (Sigma) in PBS (pH 6.5) containing 2 mM N-acetyl cysteine (Sigma) and 2 mM EDTA (ACROS Organics, Geel, Belgium) for 18 h at 60°C. GAG content was quantified using a Blyscan GAG assay (Bicolor, Westbury, NY, USA), based on 1,9-dimethylmethyl blue binding. Total collagen was quantified after hydrolyzing samples with 2 N NaOH for 20 min at 110°C using chloramine-T hydroxyproline assay with Sircol collagen standards (Bicolor). Cellularity was quantified using a Quant-iT Picrogreen double-stranded deoxyribonucleic acid (DNA) assay kit (Invitrogen, Carlsbad, CA, USA).

Sandwich enzyme-linked immunosorbent assays (ELISA) were used to detect types I and II collagen. Lyophilized samples were resuspended in 0.05 M acetic acid (Fisher Scientific) containing 0.5 M NaCl (pH 3.0) and digested with constant agitation in 10 mg/ml pepsin (Sigma) in 0.05 M acetic acid at 4°C for 4 days, followed by 1 mg/ml pancreatic elastase (Sigma) in 1× Tris-buffered saline (Sigma) at 4°C for 24 h. Capture antibodies (monoclonal mouse anti-porcine type I and II collagen, respectively; Chondrex Redmond, WA, USA) were incubated overnight at 4°C, 2% bovine serum albumin (Sigma) was used to block wells, samples/standards were added and incubated overnight, and detection antibodies (biotinylated monoclonal mouse anti-porcine type I and II collagen, respectively; Chondrex) were incubated overnight. Streptavidin peroxidase solution (VWR International, Radnor, PA, USA) was added, followed by tetramethylbenzidine (EMD Millipore, Billerica, MA, USA), and HCl (Sigma) was used to stop the reaction.

Mechanical Evaluation

Constructs were evaluated after 4 weeks of culture in unconfined compression and uniaxial tension. A 2-mm-diameter punch (Fisher Scientific) was taken from the center of each construct for compression testing. Using an Instron 5565 (Instron, Norwood, MA, USA), samples were preconditioned with 15 cycles of 5% compressive strain and then strained sequentially at 10% and 20% in a stress–relaxation test. A Kelvin solid viscoelastic model was fit to the data to quantify instantaneous modulus (E_i), relaxation modulus (E_r), and coefficient of viscosity (µ) at each strain level, using a custom Matlab program (MathWorks, Natick, MA, USA). Tensile testing was conducted using a Test Resources 840L (Test Resources, Shakopee, MN, USA). A second 2-mm-diameter punch was taken to form a dog bone-shaped tensile specimen. Paper tabs were used to grip the sample and to establish a consistent gauge length of 1.3 mm. Samples were elongated at a rate of 1% strain per second. Stress–strain curves were developed from the load-displacement curve, and Young's modulus (E_Y) was quantified using a custom Matlab program (MathWorks).

Statistics

To determine if aggregate duration was a significant factor, data were analyzed using one-way analysis of variance (ANOVA). Tukey's post hoc test was performed to determine specific effects of each treatment, when indicated by the F test ($p < 0.05$). Data are reported as mean ± standard deviation. Groups not sharing a common character are considered significantly different ($p < 0.05$). Values in text have been rounded to one decimal place.

RESULTS

As depicted in Figure 1, morphology was characterized, and histology was performed in monolayer, aggregates, and self-assembled neocartilage. Additionally, biochemical content and mechanical properties of self-assembled neocartilage was characterized after 4 weeks of culture.

Monolayer, Aggregate, and Self-Assembled Neocartilage Morphology

Figure 2 demonstrates the morphology of costochondral cells throughout the tissue engineering process: in monolayer, aggregates, and self-assembled constructs. In a monolayer, costochondral cells demonstrated a flattened, cobblestone morphology (Fig. 2A). Morphology was consistent across passage number. Within 48 h of aggregation, cell aggregates formed in the range of 0.3–0.7 mm in diameter (Fig. 2B). At the conclusion of each aggregate duration period, dissociated cells were self-assembled. Construct morphology varied within 48 h of self-assembly (Fig. 2C). Cells that did not undergo redifferentiation (0 day treatment) contracted, demonstrating a decreased construct diameter, unlike the 8-, 11-, 14-, and 21-day treatments.

Monolayer and Aggregate Histology

Histology was performed in a monolayer at confluence, prior to final passage, and at the conclusion of each aggregate duration (Fig. 3A, B). Cells in a monolayer stained minimally for intracellular collagen, while GAG staining was not detectable (Fig. 3A). Aggregate histology demonstrated the presence of collagen and GAGs for all treatments (Fig. 3B). Collagen staining increased with duration, while GAG staining remained generally consistent. Immunohistochemistry demonstrated the presence of type I and II collagen in all aggregates. With increasing aggregate duration, type I collagen decreased. Cell viability was quantified following aggregation (Fig. 3C). Viability
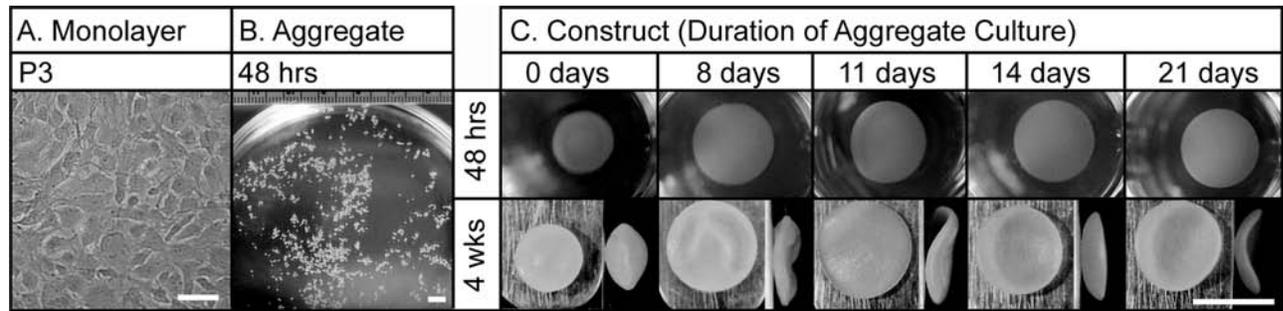
Figure 2. Gross morphology throughout neocartilage formation. (A) Cell morphology at confluence prior to P3 expansion. Scale bar: 100 ∝m. (B) Aggregate morphology after 48 h in culture. Scale bar: 5 mm. (C) Self-assembled neocartilage morphology after 48 h and 4 weeks in culture. Scale bar: 5 mm.

remained generally consistent. It was greatest after 11 days (95%) and lowest after 21 days (90%).

Neocartilage Geometry and Hydration

Diameter, wet weight, hydration, and cellularity are presented in Table 1. The 0-day treatment led to the smallest average diameter (4.0 ± 0.1 mm), while the 11-day treatment showed the largest average diameter (5.9 ± 0.2 mm). The morphology of representative constructs is depicted in Figure 2. Zero-day treatment yielded a cyst in the central region of the tissue, while 8 days yielded smaller diffuse regions in the periphery. Homogeneous, disc-shaped neocartilage was observed with 11-, 14-, and 21-day treatments. The hydration of constructs paralleled the morphology; 11-, 14-, and 21-day treatments showed decreased tissue hydration, compared with 0 and 8 days.

Neocartilage Histology and Biochemical Content

Histology reflected the presence of GAGs and collagen across all treatment groups (Fig. 4A). Picrosirius red staining in neocartilage increased as aggregate duration increased. Safranin-O staining in 8-, 11-, 14-, and 21-day treatments was increased compared with the 0-day treatment. Immunohistochemistry demonstrated decreased type I collagen as aggregate duration increased. Notably, type I collagen dropped off from 0-day treatment to 8 days, and again from 11 days to 14 days. Type II collagen staining remained generally consistent.
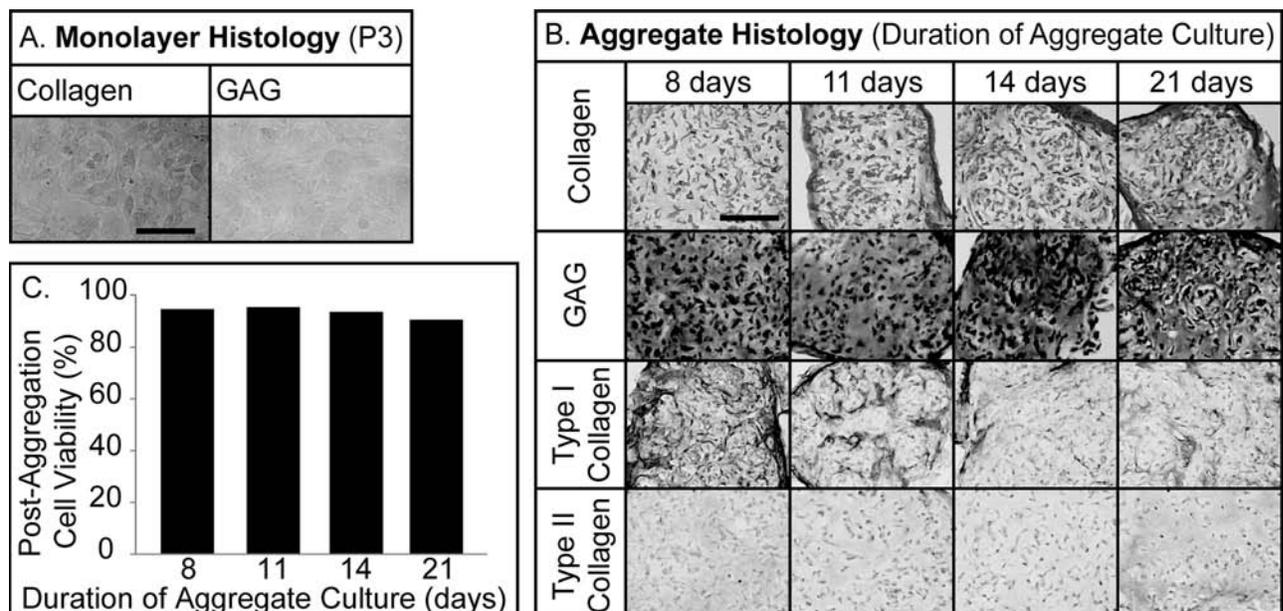
Figure 3. Monolayer and aggregate histology and cell viability. (A) Third passage monolayer cells stained minimally with picrosirius red for intracellular collagen, while Safranin-O/fast-green staining for GAGs was undetectable. Scale bar: 100 ∝m. (B) Picrosirius red and Safranin-O/fast-green staining of aggregates demonstrated the presence of extracellular collagen and GAGs, respectively, for each treatment. Immunohistochemistry for type I and II collagen demonstrated type I collagen staining that decreased with increasing aggregate duration, and the presence of type II collagen was minimal. Scale bar: 100 ∝m. (C) Cell viability varied minimally across treatments.

Table 1. Neocartilage Properties

Duration of Aggregate Culture	0 Day	8 Days	11 Days	14 Days	21 Days
Diameter (mm)	4.0 ± 0.1^c	5.6 ± 0.1^b	5.9 ± 0.2^a	5.5 ± 0.1^b	5.5 ± 0.2^b
Wet weight (mg)	19.6 ± 0.7^b	21.8 ± 2.3^a	17.1 ± 0.9^c	13.3 ± 1.3^d	12.4 ± 0.7^d
Hydration (%)	88.3 ± 0.8^{abc}	88.7 ± 0.6^a	88.5 ± 0.3^{ab}	87.4 ± 0.8^c	87.4 ± 0.8^{bc}
Cells/construct (10^6)	1.7 ± 0.1^a	1.8 ± 0.2^a	1.4 ± 0.1^b	1.3 ± 0.1^b	1.7 ± 0.2^a

Data are reported mean ± standard deviation. All groups not connected by a common letter are significantly different ($p < 0.05$).

Biochemical analysis of engineered constructs quantitatively confirmed trends observed in collagen and GAG staining (Fig. 4B, C). Collagen content increased with aggregate duration, showing significantly greater content in the 14-day ($0.8 \pm 0.09\%$) and 21-day ($0.9 \pm 0.08\%$) treatments, compared with the 0-day ($0.7 \pm 0.03\%$), 8-day ($0.7 \pm 0.05\%$), and 11-day ($0.6 \pm 0.05\%$) treatments (black bars). No significant differences were observed in GAG content between 0-, 8-, 11-, and 14-day treatments (Fig. 4C). A significant decrease was observed in the 21-day treatment. ELISA was used to quantify types I and II collagen content. Type I collagen content was below the limit of detection of the assay. Type II collagen per DNA is reported in Figure 4B (light gray bars), reflecting phenotypic alterations. The 14-day treatment significantly increased type II collagen per cell, compared with 0-day treatment. Furthermore, a trending increase was observed from 8 days to 14 days, and a trending decrease was observed from 14 days to 21 days.

Neocartilage Mechanical Properties

The tensile and compressive properties of engineered neocartilage are reported in Figure 5. Generally, the mechanical properties of the engineered tissue improved as aggregate duration increased, with no significant differences between the 14- and 21-day treatments. Young's modulus was significantly greater in the 14-day (1.3 ± 0.4 MPa) and 21-day (1.3 ± 0.3 MPa) treatments compared with the 0-, 8-, and 11-day treatments (Fig. 5A). The relaxation and instantaneous moduli in the 8-day (73.2 ± 22.1 kPa, 250.0 ± 93.5 kPa), 14-day (79.8 ± 31.8 kPa, 279.8 ± 65.7 kPa), and 21-day (77.8 ± 19.5 kPa, 347.3 ± 80.7 kPa) treatments were significantly greater than the 0-day treatments. The lowest moduli were observed in the 0- and 11-day treatments (Fig. 5B, C). Coefficient of viscosity increased with increasing aggregate duration (Fig. 5D). Both viscosity and instantaneous moduli peaked after 21 days in aggregate culture.
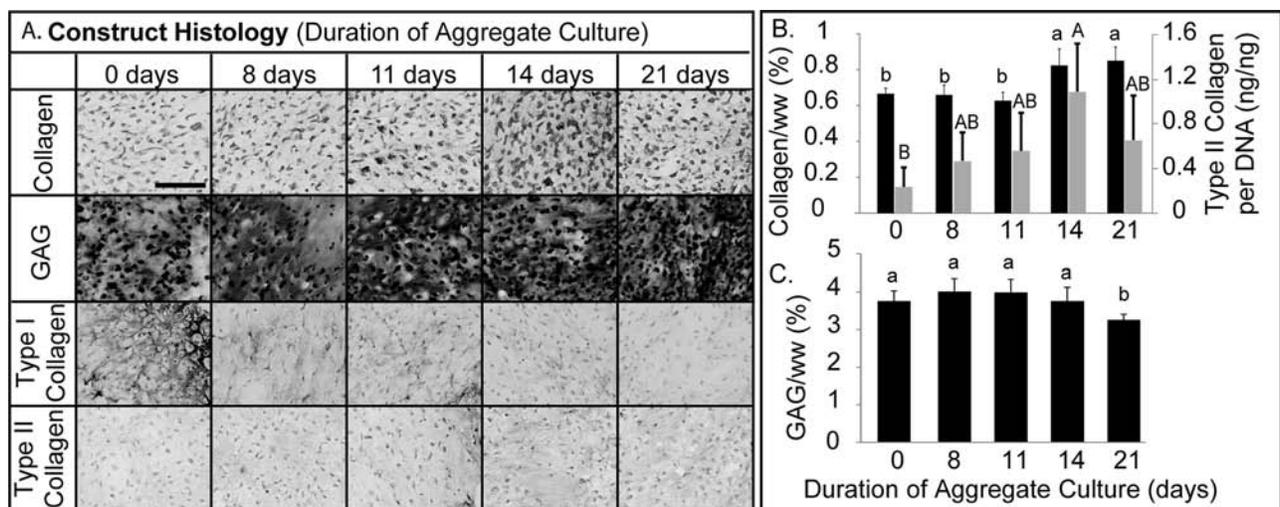
Figure 4. Self-assembled neocartilage ECM analysis. (A) Neocartilage from each treatment group was analyzed histologically for total collagen, GAGs, type I collagen, and type II collagen. Notably, GAG content varied minimally. With increasing aggregation duration, type I collagen decreased. Scale bar: 100 ∞m. (B) Neocartilage formed following 14 and 21 days of aggregation had the greatest total collagen content (dark bars), and 14 days significantly increased type II collagen synthesis per cell (light bars) compared with 0 days. Type I collagen content was evaluated quantitatively but found to be below the limit of detection of the assay. (C) GAG content did not vary appreciably up to 14 days, but decreased by 21 days of aggregation. Data are reported as mean ± standard deviation. All groups not connected by a common letter are significantly different ($p < 0.05$).
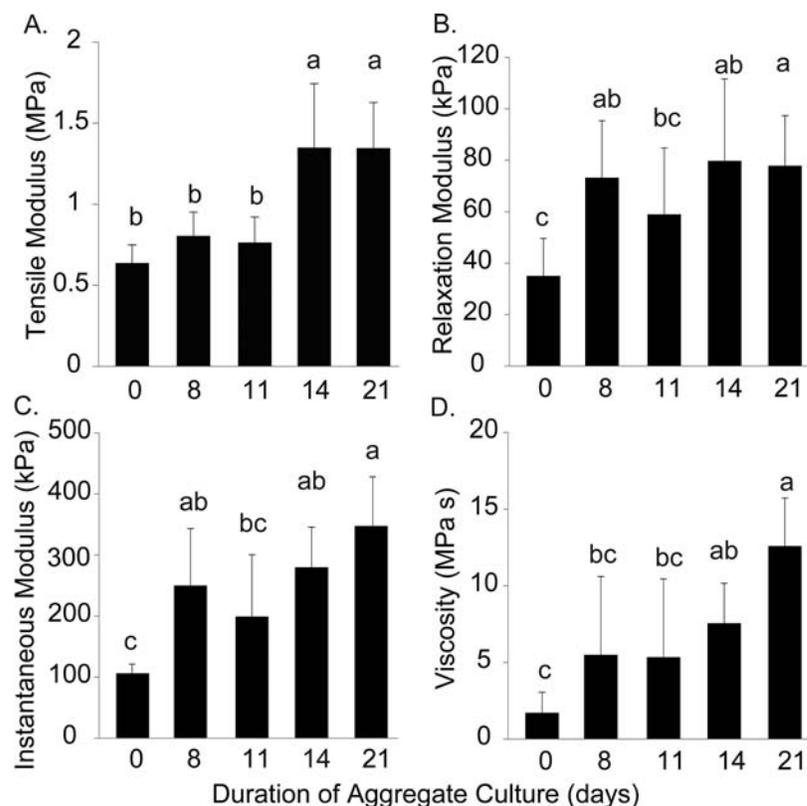
Figure 5. Self-assembled neocartilage mechanical properties. (A) Tensile modulus, (B, C) compressive relaxation and instantaneous moduli, and (D) coefficient of viscosity were measured after 4 weeks culture. Tensile stiffness increased significantly in neocartilage with 14 and 21 days of aggregation. Compressive properties increased over control in all treatments. Coefficient of viscosity was greatest with 21 days of aggregation. Data are reported as mean ± standard deviation. All groups not connected by a common letter are significantly different ($p < 0.05$).

DISCUSSION

Articular cartilages, fibrous and hyaline, are essential to load transmission throughout joint motion, and in the case of pathology, tissue engineering may present a promising therapeutic approach (25). The translational potential of tissue engineering may be improved if a spectrum of fibrous to hyaline cartilage may be engineered using a single, clinically relevant cell source. Importantly, chondrocyte expansion is associated with increased proliferation and matrix production similar to that of fibrocartilage, specifically type I collagen (13). In contrast, three-dimensional culture, following expansion, is associated with restoration of type II collagen production and matrix characteristic of hyaline cartilage (7). In the present study, the duration of aggregate culture was investigated with an objective of generating a spectrum of fibrous to hyaline self-assembled cartilage using clinically relevant costochondral cells. First, the hypothesis that increasing aggregate culture duration would increase type II to type I collagen ratio in aggregates was confirmed. Second, the hypothesis that there is a beneficial aggregate culture

duration that would increase overall collagen content, type II to type I collagen ratio, and resulting mechanical properties in neocartilage was also confirmed. However, GAG content varied only minimally with duration in both aggregates and constructs. Overall, confirming the third hypothesis, varying aggregate duration yielded a spectrum of fibrocartilaginous tissues.

Aggregate redifferentiation of costochondral cells for 8 days yielded chondrogenic matrix production as evidenced by deposition of type II collagen and GAGs and no apparent proliferation. These observations are in agreement with other aggregate culture systems. In a system utilizing aggregate culture to precondition expanded articular chondrocytes for chondrogenesis, aggregated cells demonstrated significantly decreased proliferation and increased type II collagen mRNA expression after 6 days in culture, compared with monolayer cells (44). Similarly, aggregated fourth passage chondrocytes maintained in spinner flasks demonstrated increased type II collagen and aggrecan mRNA expression within 3 days, and type II collagen increased further after 5 days (30). Eight days in

aggregate culture was sufficient to initiate the transition of costochondral cells from proliferation to chondrogenic matrix production.

Two weeks in aggregate culture further enhanced redifferentiation compared with 8 days, and the resulting cell population generated cartilage more reminiscent of hyaline cartilage. In aggregates, the most notable finding was that after 14 days, type I collagen synthesis was reduced appreciably, compared with 8 or 11 days. Previously in pellet culture, type II collagen mRNA expression peaked after 2 weeks in pellet culture, and type I collagen mRNA expression dropped appreciably from 1 week to 2 weeks and remained reduced out to 4 weeks (8). In agarose culture, it was similarly observed that after 2 weeks, only 5% of collagen peptides present were type I collagen, and the switch from type I to type II collagen was essentially complete (7). These studies demonstrate that 2 weeks in three-dimensional culture is particularly suitable for inducing a chondrogenic phenotype. Employing this regimen to engineer neocartilage significantly increased collagen content (Fig. 4) and led to a 70% increase in tensile modulus (Fig. 5). Quantified by ELISA, type II collagen synthesis increased significantly with 14-day treatment compared with 0 days and trended higher compared with 8 days (Fig. 4). The increase in type II collagen, however, did not parallel further increases in GAG content. Both engineered cartilage and articular cartilage explants cultured in vitro have historically demonstrated abundant GAG production (2). It is postulated that, in this in vitro culture system, chondrocytes are maintaining high levels of GAG production. Extending the aggregate culture to 21 days seemed to reverse the beneficial effects seen with 14 days. After 21 days in aggregate culture, aggregates showed an increase in type I collagen staining. In constructs, decreased GAG content and type II collagen were detected quantitatively. Such results demonstrate 21 days of aggregate culture exceeds the beneficial effects of redifferentiation toward a hyaline cartilage phenotype observed in the 14-day treatment.

Regulators of cell shape and cytoskeletal dynamics likely play an important role in the shift in costochondral cell phenotype observed from monolayer to three-dimensional aggregate culture. As described, a phenotypic transition was observed from proliferation in monolayer, with minimal matrix secretion, to cartilage-specific matrix production in aggregate culture. Mediated by cytoskeletal organization and interactions with the ECM, cell shape has been indicated in regulation of proliferation, differentiation, and gene expression (10,12). In both mesenchymal precursors (48) and differentiated chondrocytes (37, 43), cytoskeletal modulators affect chondrogenic differentiation and cartilage-specific matrix production (19). Specifically, the Ras homolog gene family, member A (RhoA)/Rho-associated, coiled-coil containing protein kinase (ROCK) signaling pathway and actin dynamics have been shown to play an important role in chondrocyte phenotype (45). RhoA overexpression in the chondrogenic cell line ATDC5 (derived from the mouse teratocarcinoma stem cell line AT805) has been associated with cell spreading, stress fiber formation, and increased proliferation (43,46). In micromass, RhoA/ROCK signaling inhibition resulted in increased sex-determining region Y box 9 (Sox9) mRNA expression and GAG content. Considering the change in cell morphology from adherent monolayer to nonadherent aggregate culture, it is likely cell shape and cytoskeletal mediators contributed to the decreased proliferation and increased chondrogenic matrix production observed in aggregates.

The morphology of fibrocartilage self-assembled in the 0-day and 8-day treatments may result from a heterogeneous population of chondrocytes and fibroblasts segregating based on the differential adhesion hypothesis. In constructs self-assembled from the 0-day treatment, an acellular cyst was observed in the central region that stained intensely for type I collagen, while type II collagen staining was more concentrated in the tissue periphery. In the 8-day treatment, smaller acellular regions were present, and type I collagen was localized to the acellular regions, while type II collagen was more diffuse throughout the tissue. It is suggested that a nonhomogeneous cell population is present, resulting from progressive dedifferentiation in monolayer and redifferentiation in three-dimensional culture. Assessment of phenotypic changes in sequential passage of chondrocytes demonstrates a progressive decrease in collagen type II to collagen type I gene expression with increasing passage number, commencing as early as first passage (13). Similarly, this work demonstrates progressive, time-dependent redifferentiation in aggregate culture. The nonuniform matrix distribution in these two groups suggests that the chondrocytes and fibroblastic cells migrate and segregate during self-assembly, through cadherin-mediated processes. Cadherins modulate cell sorting, migration, and adhesion during morphogenesis (18), and N-cadherin expression has been shown to peak within the first 4 days of the self-assembling process. Based upon the differential adhesion hypothesis, it is conceivable that inhomogeneous cell populations migrate and segregate, reducing the free energy associated with the cadherin-based cell–cell interactions (16). Increasing redifferentiation beyond 8 days yielded dense, homogeneous tissues, likely resulting from a more uniform chondrocyte population for self-assembly. The morphology of fibrocartilage self-assembled without redifferentiation may result from cell migration and segregation, guided by the differential adhesion hypothesis.

Aggregate culture duration may be manipulated to develop a spectrum of cartilage from a single cell source. It was found that constructs with 0-day treatment demonstrated the most intense type I collagen staining. Inversely,

constructs with the 14-day treatment had the greatest amount of type II collagen. Total collagen and tensile modulus also increased significantly with increasing aggregate duration. From 11 to 14 days, a 30% increase in total collagen and a 75% increase in tensile modulus were observed. Based upon minimal variability in cell viability, it is suggested that this transition results from progressively more cells chondrodifferentiating with time. In previous efforts to develop a fibrocartilaginous spectrum, cocultures of articular chondrocytes (ACs) and meniscus fibrochondrocytes (MCs) have demonstrated similar results. Seeding constructs with a greater proportion of articular chondrocytes (50:50 MC/AC compared with 75:25 MC/AC) increased collagen content and tensile properties (32). Additionally, in the differentiation of human embryonic stem cells (hESCs), fibrochondrocyte cocultures have been used in conjunction with growth factors to engineer fibrocartilage. Combining TGF- 3 and bone morphogenetic protein 4 (BMP-4) with differentiation cues from hESCs/fibrochondrocyte coculture resulted in a trend of increased GAG and collagen synthesis over growth factor, or coculture stimulation alone (21). In the present study, a single cell population was expanded and redifferentiated for variable durations to engineer a spectrum of fibrous to hyaline cartilage.

Neocartilage engineered in the present study demonstrated ECM content and mechanical properties approaching those of native cartilage. Neocartilage self-assembled following 8 days in aggregate culture was more fibrous in nature. The tissue demonstrated a greater proportion of type I collagen within the matrix (Fig. 4). Mechanical properties and tissue morphology were enhanced compared with neocartilage self-assembled without redifferentiation (0 days) (Fig. 5). The 8-day redifferentiation yielded a fibrocartilage similar to TMJ condylar cartilage, which demonstrates the presence of both types I and II collagen, depending upon the zone. Previously, porcine condylar cartilage has demonstrated anisotropic tensile properties with Young's modulus in the range of 6–9 MPa (28) and an apparent aggregate modulus of 75 kPa (31), compared with a Young's modulus of 0.8 MPa and a relaxation modulus of 73 kPa measured here in the 8-day treatment. In contrast, hyaline bovine articular cartilage has previously demonstrated predominantly type II collagen, tensile properties in the range of 5–8 MPa (15), and aggregate moduli in the range of 400–500 kPa (4), similar to tissue self-assembled following 14 days in aggregate redifferentiation, which demonstrated predominantly type II collagen, a tensile modulus of 1.5 MPa, and a compressive relaxation modulus of 80 kPa (Figs. 4, 5). Engineering a spectrum of fibrocartilage additionally depends upon phenotype stability with long-term in vitro culture and upon in vivo implantation. Investigation of long-term phenotypic stability in three-dimensional culture in vitro has demonstrated that primary bovine articular chondrocytes maintain their phenotype, continuing to produce type II collagen and aggrecan after 8 months of alginate encapsulation (20). Additionally, in an investigation of chondrocyte phenotype following 28 days of in vivo subcutaneous implantation, primary chondrocytes seeded in agarose gels continued to produce primarily type II collagen. No significant differences were observed in total collagen or GAG content following 28 days of implantation (42). Literature suggests the stability of the chondrocyte phenotype in extended three-dimensional in vitro culture, and upon in vivo implantation, enhancing the translational potential of the neocartilage spectrum engineered here.

CONCLUSION

A range of fibrous to hyaline neocartilage was generated using a single, clinically relevant cell source: costochondral cells. Within 8 days in aggregate redifferentiation, proliferation ceased and chondrogenic matrix production increased, compared with monolayer cells. Neocartilage formed following 14 days of redifferentiation demonstrated a 25% increase in collagen content, 100% increase in tensile modulus, and over 50% increase in compressive moduli, compared with tissue formed in the absence of redifferentiation. Increasing the aggregate duration from 8 days to 14 days yielded a spectrum of robust tissue with ECM paralleling that of fibrous TMJ condylar cartilage and hyaline femoral cartilage, respectively. Further work may turn toward approaches in tendon and ligament engineering to improve the strategy for developing homogeneous type I collagen-rich fibrocartilage, for example, the knee meniscus and TMJ disc. Additionally, future efforts to engineer hyaline cartilage may combine 14 days of aggregate redifferentiation with anabolic or catabolic stimuli in the self-assembling process to improve maturational growth.

REFERENCES

1. Anderson, D. E.; Athanasiou, K. A. Passaged goat costal chondrocytes provide a feasible cell source for temporomandibular joint tissue engineering. Ann. Biomed. Eng. 36(12): 1992–2001; 2008.
2. Asanbaeva, A.; Masuda, K.; Thonar, E. J.; Klisch, S. M.; Sah, R. L. Mechanisms of cartilage growth: Modulation of balance between proteoglycan and collagen in vitro using chondroitinase ABC. Arthritis Rheum. 56(1):188–198; 2007.
3. Athanasiou, K. A. Articular cartilage. Boca Raton, FL: CRC Press/Taylor & Francis; 2013.
4. Athanasiou, K. A.; Rosenwasser, M. P.; Buckwalter, J. A.; Malinin, T. I.; Mow, V. C. Interspecies comparisons of in situ intrinsic mechanical properties of distal femoral cartilage. J. Orthop. Res. 9(3):330–340; 1991.
5. Aulthouse, A. L.; Beck, M.; Griffey, E.; Sanford, J.; Arden, K.; Machado, M. A.; Horton, W. A. Expression of the

human chondrocyte phenotype in vitro. In Vitro Cell Dev. Biol. 25(7):659–668; 1989.

6. Barbero, A.; Grogan, S.; Schafer, D.; Heberer, M.; Mainil-Varlet, P.; Martin, I. Age related changes in human articular chondrocyte yield, proliferation and post-expansion chondrogenic capacity. Osteoarthritis Cartilage 12(6):476–484; 2004.

7. Benya, P. D.; Shaffer, J. D. Dedifferentiated chondrocytes reexpress the differentiated collagen phenotype when cultured in agarose gels. Cell 30(1):215–224; 1982.

8. Bernstein, P.; Dong, M.; Corbeil, D.; Gelinsky, M.; Gunther, K. P.; Fickert, S. Pellet culture elicits superior chondrogenic redifferentiation than alginate-based systems. Biotechnol. Prog. 25(4):1146–1152; 2009.

9. Binette, F.; McQuaid, D. P.; Haudenschild, D. R.; Yaeger, P. C.; McPherson, J. M.; Tubo, R. Expression of a stable articular cartilage phenotype without evidence of hypertrophy by adult human articular chondrocytes in vitro. J. Orthop. Res. 16(2):207–216; 1998.

10. Bissell, M. J.; Hall, H. G.; Parry, G. How does the extracellular matrix direct gene expression? J. Theor. Biol. 99(1):31–68; 1982.

11. Centers for Disease Control and Prevention. Prevalence of doctor-diagnosed arthritis and arthritis-attributable activity limitation – United States, 2007–2009. MMWR Morb. Mortal Wkly. Rep. 59(39):1261–1265; 2010.

12. Daniels, K.; Solursh, M. Modulation of chondrogenesis by the cytoskeleton and extracellular matrix. J. Cell Sci. 100 (Pt 2):249–254; 1991.

13. Darling, E. M.; Athanasiou, K. A. Rapid phenotypic changes in passaged articular chondrocyte subpopulations. J. Orthop. Res. 23(2):425–432; 2005.

14. Dolwick, M. F. The role of temporomandibular joint surgery in the treatment of patients with internal derangement. Oral Surg. Oral Med. Oral Pathol. Oral Radiol. Endod. 83(1):150–155; 1997.

15. Eleswarapu, S. V.; Responte, D. J.; Athanasiou, K. A. Tensile properties, collagen content, and crosslinks in connective tissues of the immature knee joint. PLoS One 6(10): e26178; 2011.

16. Foty, R. A.; Steinberg, M. S. The differential adhesion hypothesis: A direct evaluation. Dev. Biol. 278(1):255–263; 2005.

17. Furukawa, K. S.; Imura, K.; Tateishi, T.; Ushida, T. Scaffold-free cartilage by rotational culture for tissue engineering. J. Biotechnol. 133(1):134–145; 2008.

18. Gonsalves, K. E. Biomedical nanostructures. Hoboken, NJ: Wiley-Interscience; 2008.

19. Haudenschild, D. R.; Chen, J.; Steklov, N.; Lotz, M. K.; D'Lima, D. D. Characterization of the chondrocyte actin cytoskeleton in living three-dimensional culture: Response to anabolic and catabolic stimuli. Mol. Cell Biomech. 6(3):135–144; 2009.

20. Hauselmann, H. J.; Fernandes, R. J.; Mok, S. S.; Schmid, T. M.; Block, J. A.; Aydelotte, M. B.; Kuettner, K. E.; Thonar, E. J. Phenotypic stability of bovine articular chondrocytes after long-term culture in alginate beads. J. Cell Sci. 107 (Pt 1):17–27; 1994.

21. Hoben, G. M.; Willard, V. P.; Athanasiou, K. A. Fibrochondrogenesis of hESCs: Growth factor combinations and cocultures. Stem Cells Dev. 18(2):283–292; 2009.

22. Hu, J. C.; Athanasiou, K. A. A self-assembling process in articular cartilage tissue engineering. Tissue Eng. 12(4):969–979; 2006.

23. Huey, D. J.; Athanasiou, K. A. Alteration of the fibrocartilaginous nature of scaffoldless constructs formed from leporine meniscus cells and chondrocytes through manipulation of culture and processing conditions. Cells Tissues Organs 197(5):360–371; 2013.

24. Huey, D. J.; Athanasiou, K. A. Maturational growth of self-assembled, functional menisci as a result of TGF-beta1 and enzymatic chondroitinase-ABC stimulation. Biomaterials 32(8):2052–2058; 2011.

25. Huey, D. J.; Hu, J. C.; Athanasiou, K. A. Unlike bone, cartilage regeneration remains elusive. Science 338(6109):917–921; 2012.

26. Jakob, M.; Demarteau, O.; Schafer, D.; Hintermann, B.; Dick, W.; Heberer, M.; Martin, I. Specific growth factors during the expansion and redifferentiation of adult human articular chondrocytes enhance chondrogenesis and cartilaginous tissue formation in vitro. J. Cell Biochem. 81(2):368–377; 2001.

27. Kalpakci, K. N.; Willard, V. P.; Wong, M. E.; Athanasiou, K. A. An interspecies comparison of the temporomandibular joint disc. J. Dent. Res. 90(2):193–198; 2011.

28. Kang, H.; Bao, G.; Dong, Y.; Yi, X.; Chao, Y.; Chen, M. [Tensile mechanics of mandibular condylar cartilage]. Hua Xi Kou Qiang Yi Xue Za Zhi 18(2):85–87; 2000.

29. Kurosawa, H.; Fukubayashi, T.; Nakajima, H. Load-bearing mode of the knee joint: Physical behavior of the knee joint with or without menisci. Clin. Orthop. Relat. Res. (149):283–290; 1980.

30. Lee, T. J.; Bhang, S. H.; La, W. G.; Yang, H. S.; Seong, J. Y.; Lee, H.; Im, G. I.; Lee, S. H.; Kim, B. S. Spinner-flask culture induces redifferentiation of de-differentiated chondrocytes. Biotechnol. Lett. 33(4):829–836; 2011.

31. Lu, X. L.; Mow, V. C.; Guo, X. E. Proteoglycans and mechanical behavior of condylar cartilage. J. Dent. Res. 88(3):244–248; 2009.

32. MacBarb, R. F.; Makris, E. A.; Hu, J. C.; Athanasiou, K. A. A chondroitinase-ABC and TGF-beta1 treatment regimen for enhancing the mechanical properties of tissue-engineered fibrocartilage. Acta Biomaterialia 9(1):4626–4634; 2013.

33. Minas, T.; Nehrer, S. Current concepts in the treatment of articular cartilage defects. Orthopedics 20(6):525–538; 1997.

34. Murphy, M. K.; Huey, D. J.; Reimer, A. J.; Hu, J. C.; Athanasiou, K. A. Enhancing post-expansion chondrogenic potential of costochondral cells in self-assembled neocartilage. PLoS One 8(2):e56983; 2013.

35. Nagata, S. Modification of the stages in total reconstruction of the auricle: Part I. Grafting the three-dimensional costal cartilage framework for lobule-type microtia. Plast. Reconstr. Surg. 93(2):221–230; 1994.

36. Natoli, R. M.; Responte, D. J.; Lu, B. Y.; Athanasiou, K. A. Effects of multiple chondroitinase ABC applications on tissue engineered articular cartilage. J. Orthop. Res. 27(7):949–956; 2009.

37. Newman, P.; Watt, F. M. Influence of cytochalasin D-induced changes in cell shape on proteoglycan synthesis by cultured articular chondrocytes. Exp. Cell Res. 178(2):199–210; 1988.

38. Ofek, G.; Revell, C. M.; Hu, J. C.; Allison, D. D.; Grande-Allen, K. J.; Athanasiou, K. A. Matrix development in self-assembly of articular cartilage. PLoS One 3(7):e2795; 2008.

39. Ontell, F. K.; Moore, E. H.; Shepard, J. A.; Shelton, D. K. The costal cartilages in health and disease. Radiographics 17(3):571–577; 1997.

40. Stewart, M. C.; Saunders, K. M.; Burton-Wurster, N.; Macleod, J. N. Phenotypic stability of articular chondrocytes in vitro: The effects of culture models, bone morphogenetic protein 2, and serum supplementation. J. Bone Miner. Res. 15(1):166–174; 2000.

41. Takigawa, M.; Shirai, E.; Fukuo, K.; Tajima, K.; Mori, Y.; Suzuki, F. Chondrocytes dedifferentiated by serial monolayer culture form cartilage nodules in nude mice. Bone Miner. 2(6):449–462; 1987.

42. Vinardell, T.; Sheehy, E. J.; Buckley, C. T.; Kelly, D. J. A comparison of the functionality and in vivo phenotypic stability of cartilaginous tissues engineered from different stem cell sources. Tissue Eng. Part A 18(11–12):1161–1170; 2012.

43. Wang, G.; Woods, A.; Sabari, S.; Pagnotta, L.; Stanton, L. A.; Beier, F. RhoA/ROCK signaling suppresses hypertrophic chondrocyte differentiation. J. Biol. Chem. 279(13): 13205–13214; 2004.

44. Wolf, F.; Candrian, C.; Wendt, D.; Farhadi, J.; Heberer, M.; Martin, I.; Barbero, A. Cartilage tissue engineering using pre-aggregated human articular chondrocytes. Eur. Cell Mater. 16:92–99; 2008.

45. Woods, A.; Beier, F. RhoA/ROCK signaling regulates chondrogenesis in a context-dependent manner. J. Biol. Chem. 281(19):13134–13140; 2006.

46. Woods, A.; Wang, G.; Beier, F. RhoA/ROCK signaling regulates Sox9 expression and actin organization during chondrogenesis. J. Biol. Chem. 280(12):11626–11634; 2005.

47. Zalzal, G. H.; Cotton, R. T.; McAdams, A. J. The survival of costal cartilage graft in laryngotracheal reconstruction. Otolaryngol. Head Neck Surg. 94(2):204–211; 1986.

48. Zanetti, N. C.; Solursh, M. Induction of chondrogenesis in limb mesenchymal cultures by disruption of the actin cytoskeleton. J. Cell Biol. 99(1 Pt 1):115–123; 1984.